OPEN ACCESS
Advances in Animal and Veterinary Sciences
Research Article

Alterations of VEGF Expression and Ovarian Follicles in Doxorubicin Treated Rats: Role of Curcumin Selenium Nanoparticles

Rawya Shakir Mohammed*, Baraa Najim Al-Okaily

Department of Physiology, Biochemistry and Pharmacology, College of Veterinary Medicine, University of Baghdad, Baghdad, Iraq.

Abstract | This study aimed to investigate the protective effects of synthesized curcumin-selenium nanoparticles (CurSeNPs) by combining sodium hydrogen selenite with a hydroalcoholic extract obtained from *Curcuma longa* rhizomes in alleviating the disturbance of vascular endothelial growth factor (VEGF) mRNA expression, histomorphometric and histological alterations of ovaries in healthy rats that administered doxorubicin.Thirty-two fully grown female rats were randomly divided into four equal groups and were treated for two weeks as follows: The control group (C) of rats were administered distilled water orally ; Group G1: Rats in the this group had injected intraperitoneal of doxorubicin (4.40mg/kg B.W), (Group 2): Rats were intraperitoneally injected with CurSeNPs (10.47 µg/kg B.W.), in contrast, both Doxorubicin and CurSeNPs were administered to Group 3 at the same doses. Ovarian tissue specimens have been taken to determine the level of ovarian VEGF mRNA gene expression, as well as for a histological study. The results showed a significant rise in VEGF gene expression levels, as well as the presence of histological alterations in the G1 group characterized by clear congestion of graffiti follicles and necrotic lesions. with decrease in the number of primary, secondry and graafian follicles as compared to other groups. Nevertheless, current results indicated that the administration of CurSeNPs with or without doxorubicin in the G2 and G3 groups revealed a decrease in the expression of the VEGF gene and an improvement in the inflammatory lesions of ovaries.The current study has demonstrated that CurSeNPs exhibit preventive effects against doxorubicin toxic effects in healthy adult female rats, which may be due to their antioxidant, anti-inflammatory, and anticancer activities.

Keywords | Curcumin, Doxorubicin, Ovarian follicles, Selenium nanoparticles, VEGF gene, Rats

Received | July 12, 2024; **Accepted** | July 26, 2024; **Published** | October 05, 2024
***Correspondence** | Rawya Shakir Mohammed, Department of Physiology, Biochemistry and Pharmacology, College of Veterinary Medicine, University of Baghdad, Baghdad, Iraq; **Email:** rawia.mirza2106p@covm.uobaghdad.edu.iq
Citation | Mohammed RS, Al-Okaily BN (2024). Alterations of VEGF expression and ovarian follicles in doxorubicin treated rats: role of curcumin selenium nanoparticles. Adv. Anim. Vet. Sci. 12(11): 2185-2194.
DOI | https://dx.doi.org/10.17582/journal.aavs/2024/12.11.2185.2194
ISSN (Online) | 2307-8316; **ISSN (Print)** | 2309-3331

INTRODUCTION

Green nanoparticle synthesis has great potential in the biomedical and environmental scientific fields (Jadoun *et al*., 2021). The green chemistry method promotes the utilization of plants and plant extracts, providing a credible, uncomplicated, non-toxic, cost-effective, stable, and environmentally friendly method (Sood and Khudiar, 2019; Wali and Alqayim, 2019). Selenium is an essential trace mineral for an individual's body, with properties of

both minerals and nonmetallic compounds. Selenium exhibits biological characteristics associated with the immune system, antioxidation, antiviral activity, and anticancer activities (Zhou *et al*., 2020). Additionally, selenium nanoparticles (SeNPs) have the ability to reduce and alleviate heavy metal toxicity. They offer advantages such as a high absorption rate, increased biological activity, and lower toxicity levels (Zhang *et al*., 2023).

The SeNPs s demonstrates efficacy in decreasing the rate of cancer cell growth (Geoffrion *et al*., 2020). Because, the stability of these nanoparticles is enhanced by their unique organic molecule covering, which effectively inhibits any gradual buildup over time (Wali and Alqayim, 2019; Shareef *et al*., 2024). The black currant selenium nanoparticle works as an antioxidant. It exhibits both prophylactic and therapeutic properties in mitigating the harmful impact of D-galactose (Khudair *et al*., 2020). Also, *Avena sativa* seed crude extract protects the heart from DOX-induced toxicity in rats (Salim and Hasan, 2022). Curcumin is a polyphenolic substance that is naturally found in the rhizome of *Curcuma longa* (Patel *et al*., 2020). Besides, curcumin demonstrates notable multi-pharmacological capabilities, including anti-tumor and anti-inflammatory activities (Peng *et al*., 2021). Curcumin phytosome nanoparticles have the capacity to lower inflammation and decrease cholesterol levels, as proven by Jadaan and Khudair, 2023. Additional research has provided further evidence to support the concept that phytochemicals play a vital role in controlling the creation of metal nanoparticles (Al-Kurdy and Khudair, 2020).The anticancer effects of curcumin on ovarian cancer act through various mechanisms, including disrupting cellular interactions essential for the spread and recurrence of ovarian cancer cells, enhancing the production of pro-apoptotic proteins, and regulating the generation of various molecules such as cytokines, transcription factors, enzymes, protein kinases, and growth factors (Bhatia *et al*., 2021) .These nanoparticles have potential applications in several fields such as medicine and therapy (Jaffar and Hussein, 2015). Doxorubicin, a type of medication used to treat various tumors, has been related to adverse effects and toxicity in crucial organs, particularly cardiotoxicity (Dulf *et al*., 2023), in addition ovarian toxicity, which is manifested by decreased ovulation and associated with a decrement in ovarian size, caused probably by ovarian injury (Gao *et al*., 2023).DOX caused damage to actively dividing granulosa cells in the ovary, resulting in the programmed cell death of follicles and ultimately disrupting female ovarian activity and ovulation (Xiao *et al*., 2017). DOX has harmful effects on ovarian follicles in rodents, such as follicular atresia, excessive activation (Wang *et al*., 2019), and decreased synthesis of 17beta-estradiol (E2) (Xiao *et al*., 2017). Therefore, this study was conducted to examine modern approaches for manufacturing and analyzing CurSeNPs and their ability to lower the possible hazards of doxorubicin exposure on several reproductive aspects of the ovaries in healthy adult female rats.

MATERIAL AND METHODS

Preparation of CurSeNPs

Curcuma longa alcoholic extract was prepared as described by Jayarambabu *et al*. (2020) using a magnetic stirrer. The rhizomes were dried, pulverized, and mixed with ethanol for six hours at 70-80°C. The alcohol was extracted using a rotary evaporator. Selenium nanoparticles were created by mixing sodium hydrogen selenite with distilled water, subjected to sonication, and stored in a dark place. The alcoholic extract of Curcuma longa was used as an efficient reducing agent to synthesize CurSeNPs) from sodium selenite (0.04M). The extract were then added dropwise to the selenite solution, stirring for four hours. The color changed from lighter orangish-red to deeper orangish-red, and a dark orange-red color was observed. The solution was then spun at 10,000 rpm for 20 minutes, centrifuged at 6,000 rpm for 15 minutes, and iterated three times to eliminate organic impurities. The SeNPs were dried at 45 °C. (Al-Ebadi *et al*., 2021).

Characterization of CurSeNPs

Characterization of CurSeNPs was performed by: Ultraviolet– visible spectroscopy (Metertech SP-8001 Taiwan) as described by Soleimani *et al*. (2018); X-ray diffraction (Shemadzu-6000 Japan)as describe by Fouda *et al*. (2022), Fourier-transform infrared spectroscopy (Shimadzu8400s, Japan), this method is likely comes from the research by Al-Kurdy and Khudair, (2020) Zeta potential and Field emission scanning electron microscope (FE-SEM) (SEM-Tescan Vega III, Czech) and atomic force microscopy(AFM) (TOSHIBA/Japan).

In Vivo Study of CurSeNPs

The current study was conducted at an animal house at the College of Veterinary Medicine / University of Baghdad. The study's use of animals got ethical approval by the local committee of animal care and use (P.G. 2641 date 29-11-2023). Thirty-two adult healthy female wistar rats were utilized in this investigation. After the acclimatization phase, they were randomly and evenly divided into four experimental groups. These groups were subjected to the given treatment for a duration of two weeks: Rats in control group (C) were orally delivered distilled water, Group G1: Rats in the this group had injected intraperitoneal of doxorubicin (STADA /Germany) at a dose of 4.40mg/kg B.W, G2 group, Rats administered CurSeNPs at a dose of 10.47 µg/kg B.W, while both of doxorubicin and CurSeNPs at the same doses were given to G3 group. Ovarian tissue specimens were taken to measure the gene expression VGEF mRNA, and the RNA extraction kit from Genaid Korea was used to extract total RNA from the ovarian tissue. The measurement of gene expression was performed uti-

lizing the Forward primer (5'-GCACCCATGGCAGAAGG-3') and Reverse primer (5'-CTCGATTGGATGGCAGTAGCT-3') specific to the VEGF gene (Pang *et al.*, 2020). The AddScript RT-qPCR Syber master kit from AddBio, Korea was utilized for this study. The RT-qPCR findings were assessed according to the guidelines given by Schmittgen and Livak (2008). Besides, another part of the specimens was fixed in a 10% formal saline solution to preserve their structure; then the fixed tissues were embedded in paraffin wax. Thin slices, 5 micrometers thick, were cut from the paraffin blocks and the sections were A staining with hematoxylin and eosin (H and E) for pathohistological examination under a microscope according to Suvarna et al. (2018) furthermore, histomorphometric analysis of ovarian tissues were conducting (Suad *et al.*, 2018).

Statistical Analysis

The data were analyzed using SPSS version 26, and the outcomes are presented as means ± Standard deviation (SD). One-way analysis of variance (ANOVA) followed by post hoc test to compare between groups P value < 0.05 pointed a statistical significance (Baarda and van Dijkum, 2019). A post hoc multiple comparison test was employed to compare the treatment groups with the control group. An analysis of variance (ANOVA) was conducted, followed by a post hoc multiple comparison test. A probability value significance criterion of 0.05 was utilized.

RESULTS AND DISCUSSION

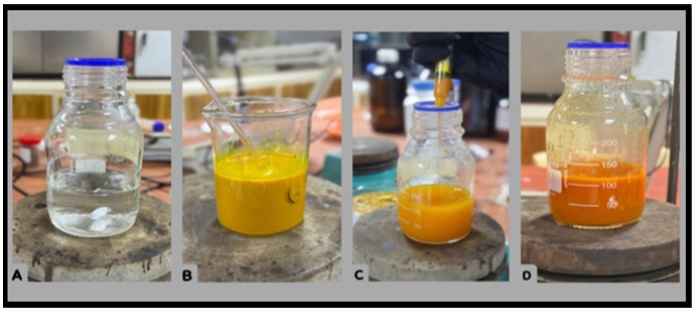

Figure 1: The image displayed the color transformation of sodium selenite into CurSeNPs by the use of an alcohol-based *Curcuma longa* extract; **A:** demonstrated a solution of sodium selenite lacking color; **B:** displayed an alcoholic extract of *Curcuma longa*; **C:** displayed curcumin selenium nanoparticles; **D:** depicted an image of CurSeNPs after a 24-hour period.

Figure 1 illustrates the gradual change in colour of the reaction mixture throughout the biosynthesis process. The formation of CurSeNPs was demonstrated by the gradual change in colour from brilliant orange to a darker orange-red shade after 40 minutes, indicating enhanced stability. The optical absorbance of *curcuma longa* extract and synthesized CurSeNPs was measured the change in the color using UV-Vis spectroscopy demonstrating that theabsorption peak between 427-214 nm confirm the presence of CurSeNPs (Figure 2). Results of FTIR of alcoholic extract of *Curcuma longa* and CurSeNPs revealed distinct bands at different peaks (Figure 3). The XRD test provides precise data on the size of nanomaterials and the crystal type present in a substance (Figure 4).

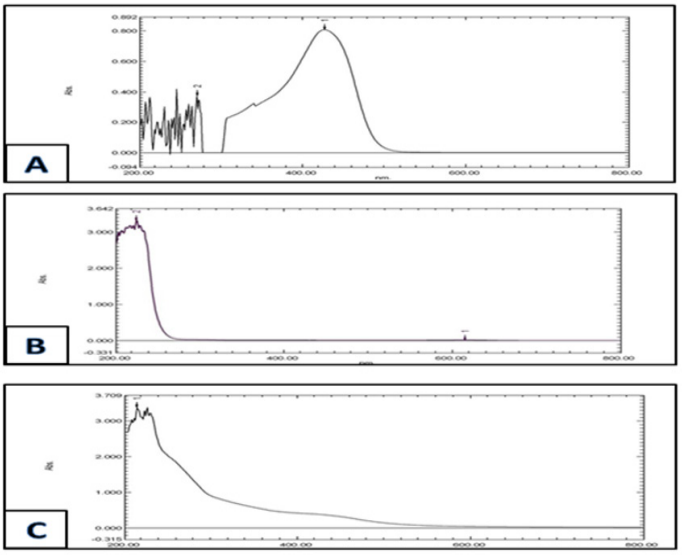

Figure 2: UV-Vis measure the absorbance of; **A:** *Curcuma longa* extract; **B:** Sodium hydrogen selenite; **C:** CurSeNPs.

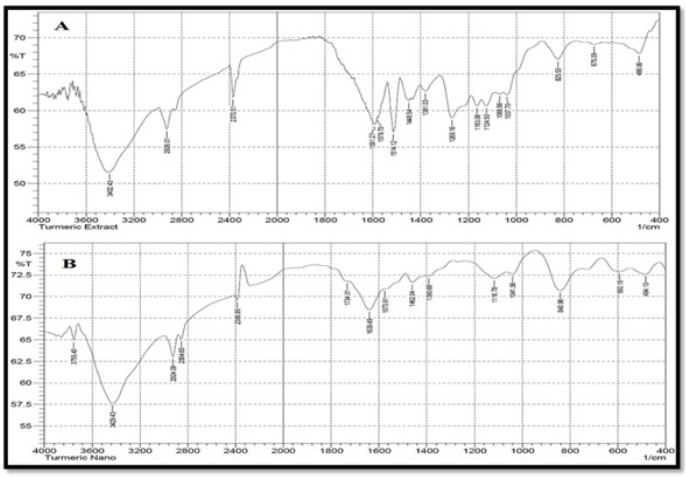

Figure 3A: The FT-IR spectra of the alcoholic extract of *Curcuma longa*; **B:** the FT-IR spectrum of the functional groups of *Curcuma longa* extract coupled to SeNPs are provided.

A zeta potential value exceeding 30 mV indicates a high level of stability (Figure 5). The pattern of FE-SEM revealed the existence of spherical, amorphous structures with diameters ranging from 21 to 37 nm (Figure 6). The atomic force microscope displays a two-dimensional view of CurSeNPs (Figure 7A). The present results demonstrated that mRNA analysis of rats' ovarian tissues (Figures 8 and 9). A notable (P<0.05) upregulation of the VEGF gene expression in group G1 compared to the other experimental groups was observed. While Following CurSeNPs administration with or without doxorubicin, rats exhibit-

ed a significant (P<0.05) reduction in VEGF expression compared to the G1 group (Figure 10). Table 1 showed a significant (p < 0.05) reduction in the number of follicles in doxorubicin treated group compared to the control group. In addition, rats that received CurSeNPs with or without doxorubicin in groups G2 and G3 showed a significant (p< 0.05) increase in the number of ovarian follicles compared to group G1. Also, (Table 2) also demonstrates the impact of injecting doxorubicin and orally intubating CurSeNPs on the diameter of ovarian follicles. The results revealed a significant (p <0.05) reduction in the diameter of all follicles in group G2 (treated with doxorubicin) compared to the control group, as well as groups G2 and G3. In addition, rats in groups G2 and G3, showed a significant (p < 0.05) increase in diameter compared to the G1 group. The ovaries of the control group show normal different type of follicles involved graafian follicles, germinal epithelium, theca layer, granulosa cell layer, oocyte, antrum and oogonium (Figure 11). Compared to the control group (Figure 11) group exhibited clear congestion of Graafian follicles with sloughing and degenerative lesion in the granulosa cell layer), The other section shows a clear necrotic lesion in the griffin follicle with lysis of oocyte, associated with clear damage and necrosis of epithelia of oogonium (Figures 12 and 13). While histological sections of group G2 (Figure 14 and 15) show graffian follicles, germinal epithelium, theca layer, Oocyte, granulosa cell layer, antrum, and Oogonium without damag. Whereas a clear blood vessels congestion of ovarian veins with infiltration of inflammatory cells in the ovarian tissue were observed in group G3 (Figure 16).

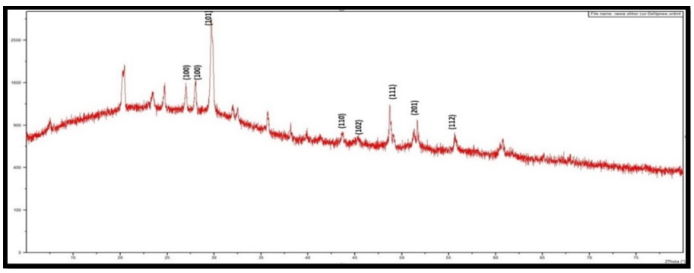

Figure 4: Sodium selenite solution and an alcoholic extract of *Curcuma longa* were used to synthesize curcumin selenium nanoparticles, which were characterized by the X-ray diffraction pattern.

The curcumin extract and sodium selenite react to affect the mixture's color. To create environmentally safe CurSeNPs,curcumin served as a reducing and stabilizing agent. Previous investigation have used a variety of green plants to generate the unique reddish-orange color of CurSeNPs nanoparticles (Sabea and Al-Qaiym, 2023).The color transition from yellow to reddish-orange upon heating serves as an indication of an increase in particle size (Figure 2A) demonstrated that the peak at 427 nm was impeded in the solution of Curcuma longa. In contrast, the solution of Cur-Se-NPs (Figure 2C) exhibited a shift from 427 to 214 nm, indicating that curcumin, the primary constituent of turmeric (*Curcuma longa*), was present (Soleimani *et al*., 2018).

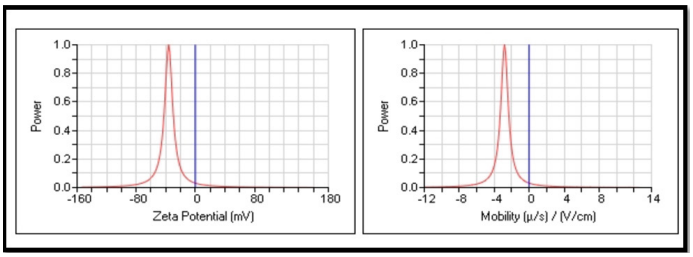

Figure 5: Zeta potentials of curcumin selenium nanoparticles A and B.

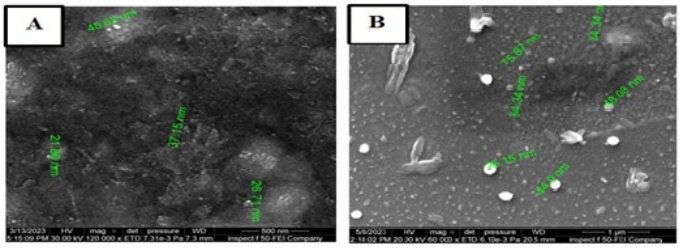

Figure 6: The FESEM image displayed the dimensions and properties of the synthesised Cur-Se-NPs, with (A) measuring 500nm and (B) measuring 1 µm.

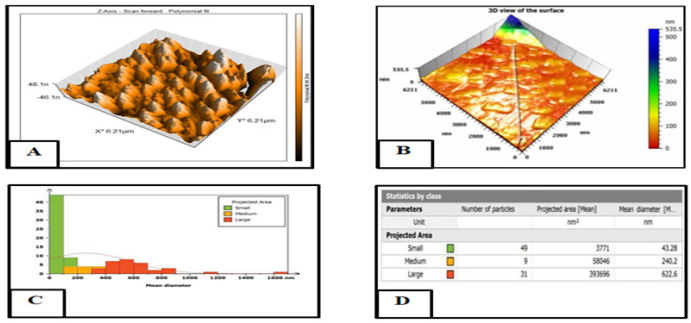

Figure 7: Atomic force microscopy (AFM) was used to analyze the size distribution of selenium nanoparticles (CurSeNPs). The results were shown in the form of a two-dimensional picture (a), a three-dimensional image (b), and a size distribution histogram (c) and (d).

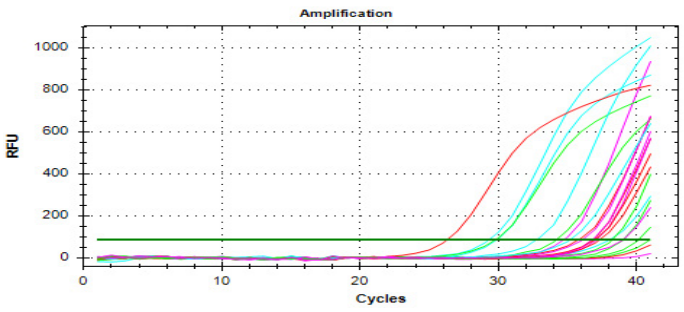

Figure 8: The real time amplification plots of VEGF gene expression of ovarian tissue in rats experimental samples. the real time PCR polts of VEGF gene. The blue plots (control group), green plots (G1 group), red plots (G2group), purple plots (G3 group).

The FT-IR spectra exhibited prominent absorption bands at (3755–3429 cm1) and indicating the presence of hydroxyl (-OH) or amine groups (-NH) (3402 cm1) in the *Curcuma longa* extract. Alternatively, CH stretch alkynes are indicated by the absorption peak at (2924, 2926 and 2854 cm–1).

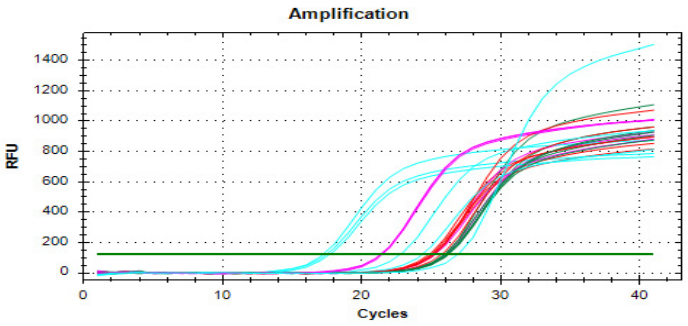

Figure 9: The real time amplification plots of housekeeping (GAPDH) gene expression of ovarian tissue in rats experimental samples. the real time PCR polts of VEGFgene. The blue plots (control group), green plots (G1 group), red plots (G2group), purple plots (G3 group).

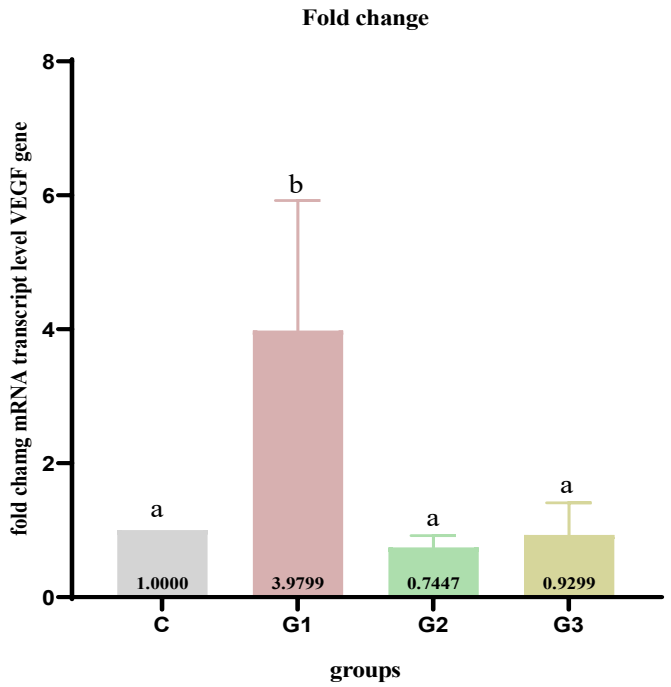

Figure 10: Assessment of VEGF gene expression in ovarian tissues of rats treated with CurSeNPs, doxorubicin and both after 14 days; *Values are expresses as mean ± SD; **n:**5; C: Control group; **G1:** Injected with i/p doxorubicin 4.40 mg /kg. b. w.; **G2:** Administrated with CurSeNPs 10.47 µg / kg bw. Orally; **G3:** Administrated with CurSeNPs 10.47 µg / kg bw; orally and with doxorubicin 4.40 mg! kg b. w. i/p.Different small letters mean significantly differences between groups $P<0.05$.

The plant extract included carbon dioxide (0 = C = 0) as indicated by the peak at wavenumbers (2385 and 2370 cm–1). Around 1734, the absorption peaks. The carboxyl groups are represented by 06 cm-1. The C=C bond is associated with the absorption peaks at 1639 cm-1.

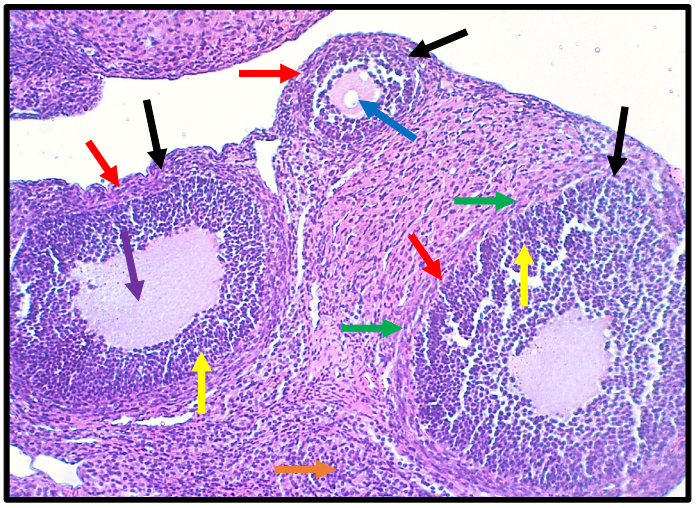

Figure 11: Histological section in ovary of rat in control group. The section shows graffian follicles (Black arrows), germinal epithelium (Red arrows), theca layer (Green arrows), granulosa cell layer (Yellow arrows), Oocyte (Blue arrow), antrum (purple arrow) and Oogonium (Orange arrow). The tissue is stained with H and E stain and the section is captured using light microscope and digital camera at 10X magnifier scale.

The N-O bond is associated with the absorption peak at 1573 cm-1, whereas the peak represents the C-H bond at 1462.04 cm-1. Concerning the S = O, the absorption peaks may be seen around 1390.68 cm-1. The stretching of the C-N bonds in the amines is shown by the absorption peaks at 1269.16 cm-1 and 1163.80, 1124.50, 1116.78, 1068.56, 1041.56 and 1037.56 cm-1. The stretching of C-X bonds in alkyl halides results in bands at 825.53, 840.96, and675.90 cm–1, whereas the bending of C-N-C bonds in amines generates the weak bands at 592.15 and 484.13 cm–1. Based on these results, it appears that there are a number of biomolecules with functional groups that might help stabilize and reduce the SeNPs. Figure 5 shows the results of Zeta potential investigation carried out on CurSeNPs, which indicates a negative surface charge range from -120 to +60, with a specific value of -36.08 mV, this is due to the polyphenolic and flavonoid parts of the reducing agent in the plant extract, which show electrostatic forces in the nanoparticles made from green materials. All particles in the synthesized solution possess a negative zeta potential value, contributing to their high stability and preventing aggregation and making them easier for cell absorption and maintaining their nanostructure integrity (Nasrollahzadeh and Sajadi, 2016). The FE-SEM pictures, seen at various magnifications, revealed the existence of spherical, amorphous structures with diameters ranging from 21 to 37 nm, as depicted in (Figure 6). The atomic force microscope displays a two-dimensional view of CurSeNPs (Figure 7A)

Table 1: Effect of CurSeNPs, doxorubicin and both on number of primary and secondary, Graafian follicle in Ovarian tissue after 14 days.

Groups/ Number of follicles	C	G1	G2	G3
Primary follicles	6.60 ± 1.140 a	2.60 ± 0.547 c	6.20 ± 1.09 a	4.00 ± 1.00 b
Secondary follicles	4.400 ± 0.89 a	1.80 ± 0.83 b	3.80 ± 0.83 a	2.6 ± 0.894 b
Graafian follicles	2.40 ± 0.89 a	0.00 ± 0.00	2.20 ± 0.83 a	1.60 ± 0.89 a

*Values are expresses as mean ± SD; **n:**5; **C:** Control group; **G1:** Injected with i/p doxorubicin 4.40 mg /kg. b. w.; **G2:** Administrated with CurSeNPs 10.47 µg / kg bw. Orally; **G3:** Administrated with CurSeNPs 10.47 µg / kg bw. orally and with doxorubicin 4.40 mg! kg b. w. i/p.; *Different small letters mean significantly differences between groups at P<0.05.

Table 2: Effect of CurSeNPs, doxorubicin and both on diameter mm of primary and secondary, Graafian follicle in Ovarian tissue after 14 days.

Groups/Diameter mm	C	G1	G2	G3
Primary follicles	14.31 ± 1.32 a	10.72 ± 1.22 c	13.76 ± 1.11 a	12.40 ± 1.03 b
Secondary follicles	25.43 1.48 a	19.79 ± 1.21 c	24.77 ±1.52 a	23.07 ±2.01 b
Graafian follicles	39.11± 0 .87 a	0.00 ± 0.00	37.76 ± 2.06 a	37.32 ± 1.22 a

*Values are expresses as mean ± SD; **n:** 5; **C:** Control group; **G1:** Injected with i/p doxorubicin 4.40 mg /kg. b. w.; **G2:** Administrated with CurSeNPs 10.47 µg / kg bw. Orally; **G3:** Administrated with CurSeNPs 10.47 µg / kg bw. orally and with doxorubicin 4.40 mg! kg b. w. i/p.; *Different small letters mean significantly differences between groups at P<0.05.

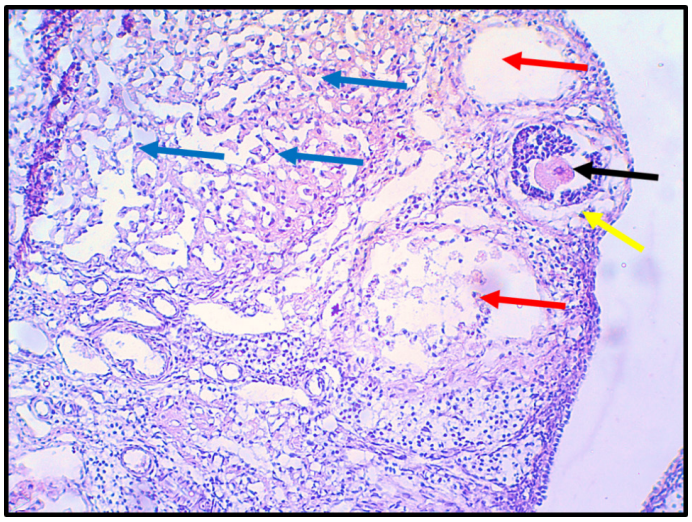

Figure 12: Histopathological section in ovary of rat that treated with doxorubicin group G1. (4.4mg./kg.b.w. for 14 days). The section shows clear congestion of graffian follicles (Oocyte, Black arrow) with sloughing and degenerative lesion in the granulosa cell layer (Yellow arrow). The section shows clear necrotic lesion in the graffian follicle with lysis of Oocyte (Red arrows). The Oogonium shows clear damage and necrosis of epithelia (Blue arrows). The tissue is stained with H&E stain and the section is captured using light microscope and digital camera at 10X magnifier scale.

which appear as clusters of spherical shapes in either isolated or aggregated forms. While, the (Figure 7B) displays a three-dimensional image of CurSeNPs, which exhibits a population of uniform particles with a smooth surface. In addition, (Figures 7C and D) demonstrated that the diameter of the synthesized curSeNPs varied between 3 and 43 nm, with a height of around 46.1n–48. The current results revealed that mRNA analysis of rats' ovarian tissues indicated upregulation of the VEGF gene expression in group G1 compared to the other experimental groups in agreement with study of Torres-Ruiz *et al.* (2023), who confirmed the upregulation of main lymphangiogenic receptor characterized with higher mRNA and protein levels of VEGFR3 after a short treatment with doxorubicin in cellular models when compared to the parental cell line. In addition, hypoxia triggers the activation of hypoxia-inducible factor 1α (HIF-1α), which manages the transcription of key molecules such as VEGF and sirtuin-1 (SIRT-1) (Pinto *et al.*, 2024). As well as that acute or chronic hypoxia caused an increase in VEGF expression and decreased the pro-angiogenic potential factors in liver cancer cells, associated with a notable activation of the ROS/NF-κB/hypoxia-inducible factor-1α/VEGF signaling pathway (Refaie *et al.*, 2022). The downregulation of VEGFR-3receptor leads to a reduction of cancer in vivo models through reduced migration and the proliferation capacities of cancer cells (Walsh *et al.*, 2022).

Rats received CurSeNPs with or without doxorubicin rats exhibited a reduction in VEGF expression compared to doxorubicin-treated rats. This result was in accordance with other studies (Elneklawi *et al.*, 2023). The chemical structure of curcumin as a phytochemical compound has been (Giordano and Tommonaro, 2019) safe and effective, and the role of curcumin as an anticancer had been widely proven. A recent study by Liu *et al.* (2023), demonstrated that curcumin decreases VEGF, activity and expression of matrix metalloproteinases (MMPs), urokinase plasminogen activator (uPA), and modulating E-Cadherin (E-Cad) leading to inhibit the metastasis in case of ovarian cancer by the effect of bisdemethoxycurcumin (BDMC) (Liu *et*

al., 2023). Besides, strawberry extract loaded within niosomes showed alleviating VEGF gene expression by improving XBP1/mRNA-21/mRNA-330 signaling pathways in rats' uterus injury induced by cisplatin (Elneklawi *et al*., 2023). Also, the effect of curcumin on VEGF expression may be via the inhibition of the NF-κB pathway and activation of the sirtuin-1 molecule (Ungurianu *et al*., 2022), in addition, it regulate of NF-kB and cyclooxygenase-2 (COX-2) (Hutomo *et al*., 2017). The anticancer effects of SeNPs and their mechanisms were well evaluated by Menon *et al*. (2018), who showed that cancer cells have an acidic pH that leads to a peroxidative and triggers an increased production of free radicals, causing leakage of mitochondrial proteins and stress of the endoplasmic reticulum resulting to triggers of apoptosis, through activation of many molecular signaling pathways for oncogenic, including MAPK/Erk, PI3K/Akt/mTOR, NFκB, Wnt/β-catenin, and apoptosis pathways, While SeNPs cause modulating and/or diminished VEGF, PI3K/Akt/mTOR, MAPK/Erk, and Wnt/β-catenin pathways by decreased cellular proliferation associated with impeding the enhancement of growth-promoting signaling in the cancer cell microenvironment. Recently, Khaledizade *et al*. (2024), showed that the expression levels of VEGF,, BCL2, MMP2, MMP9, CCNE1, CCND1, and ERBB2 were downregulated after SeNPs treatment in MCF-7 breast cancer cell line (Khaledizade *et al*., 2024). The histopathological results in group G1 were in agreement with Samare-Najaf *et al*. 2020, who showed that the administration of doxorubicin causes the development of ascites, ovarian hemorrhage, reduced number of ovarian follicles, and tissue atrophy. The study has demonstrated the impact of chemotherapy drugs on the vascular system of the ovaries with follicular loss (Regulska *et al*., 2019) is by indirectly impairing the stroma and the vascular system (Soleimani *et al*., 2011). Also, apoptosis in ovarian cells can lead to significant follicular atresia or regression and is regarded as one of the primary mechanisms responsible for ovarian aging (Yang *et al*., 2019). Besides, oxidative stress can trigger programmed cell death in ovarian germ cells through multiple mechanisms, such as external or endogenous pathways (Jalouli *et al*., 2022). Apoptosis of granulosa cells causes a lack of nutrients and triggers metabolic dysfunction in the ovarian microenvironment (Palmerini *et al*., 2016) apoptosis increases the concentration of cell-free DNA in the fluid surrounding the ovarian follicles, hence increasing the deterioration in ovarian function. The present investigation showed a positive effect of CurSeNPs and demonstrated improvement in the ovarian function of rats by enhancing histological modifications in the ovaries caused by modulation of histomorphometric analysis and histopathological changes caused by doxorubicin (group 3). This was evidenced by an improvement in folliculogenesis and a decrease in the number of atretic follicles. These findings are consistent with previous research that showed selenium supplementation can protect rat ovaries from the effects of arsenic (Alhealy et al., 2021). Current results show that polyphenols found in foods and spices, such as curcumin, gallate, epicatechin, and resveratrol, have strong anti-tumor solid effects and provide protection to the reproductive system in cancer patients (Carvalho *et al*., 2017).

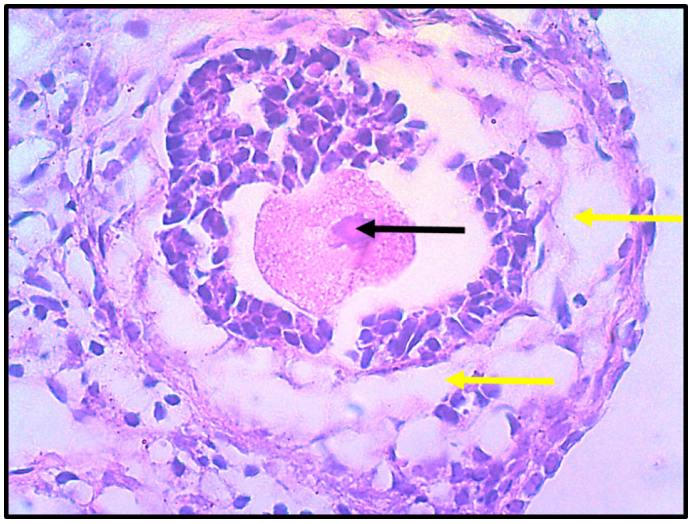

Figure 13: Histopathological section in ovary of rat that treated with doxorubicin group G1 (4.4mg./kg.b.w. for 14 days). The section shows clear congestion of graffian follicles (Oocyte, Black arrows) with sloughing and degenerative lesion in the granulosa cell layer (Yellow arrows). The tissue is stained with H and E stain and the section is captured using light microscope and digital camera at 40X magnifier scale.

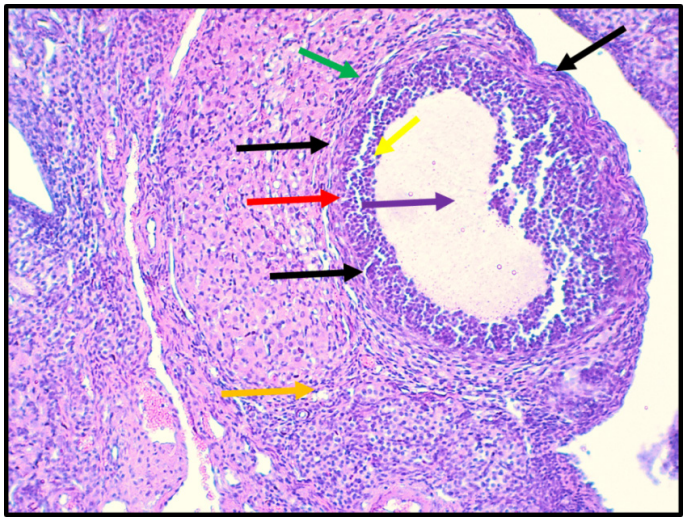

Figure 14: Histological section in ovary of rat in G2 group (CurSeNPs 10.47 µg/kg.bw.). The section shows graffian follicles (Black arrows), germinal epithelium (Red arrows), theca layer (Green arrows), granulosa cell layer (Yellow arrows), antrum (purple arrow) and Oogonium (Orange arrow). The tissue is stained with H and E stain and the section is captured using light microscope and digital camera at 10X magnifier scale.

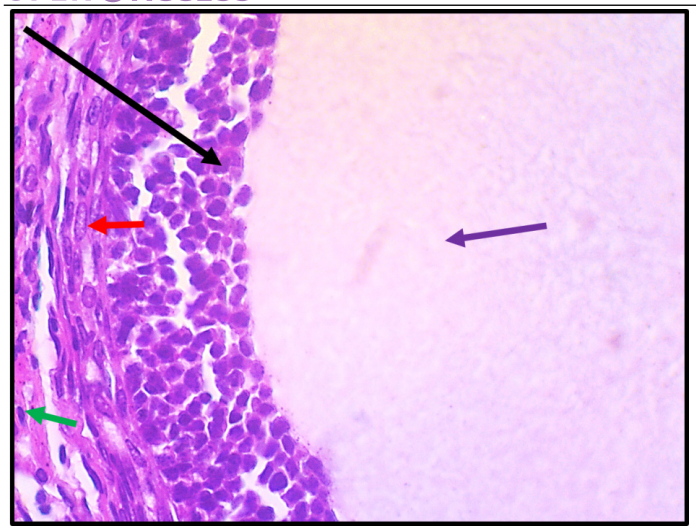

Figure 15: Histological section in ovary of rat in (G2 group, CurSeNPs 10.47 µg/kg.bw.). The section shows graffian follicles (Black arrow), germinal epithelium (Red arrow), theca layer (Green arrows) and antrum (purple arrow). The tissue is stained with H and E stain and the section is captured using light microscope and digital camera at 40X magnifier scale.

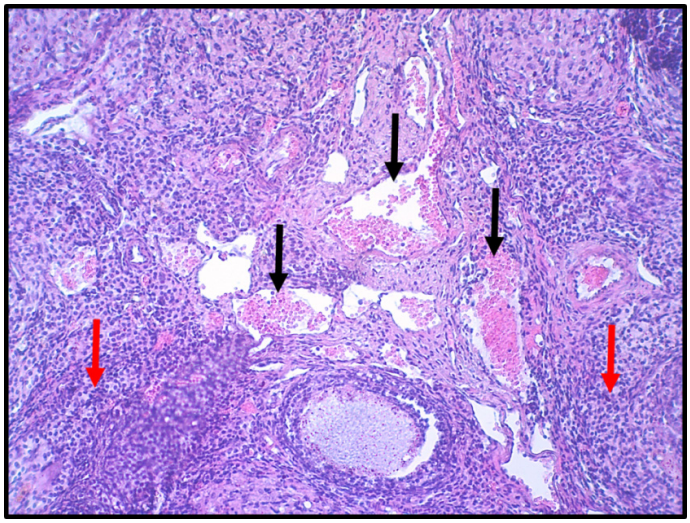

Figure 16: The histopathological section of ovary in rats of G3 group that treated with (Doxorubicin 4.40 mg /kg. b. w. + CurSeNPs 10.47 µg / kg bw.). The section sows clear blood vessels congestion of ovarian veins (Black arrows) with infiltration of inflammatory cells in theovarian tissue (Red arrows). The tissue is stained with H and E stain and the section is captured using light microscope and digital camera at 10X magnifier scale.

CONCLUSIONS AND RECOMMENDATIONS

In total, based on our knowledge, CurSeNPs can be produced biologically by employing *Curcuma longa* extract to create nanoparticles naturally. This is a simple, low-cost method that can be applied in biomedicine and has the potential to prevent or treat ovarian doxorubicin toxicity in adult female rats. This is the first study to confirm the protective effects of CuSeNPs against doxorubicin on VEGF gene expression and histological changes in the ovarian tissues of healthy female rats. The roles of CurSeNPs in regulating oestrogen receptors (ESR1 and ESR2) in both female and male rats subjected to anti-tumor medicines, as well as in mitigating the negative effects of experimentally-induced polycystic ovary and solid tumour in female rats.

ACKNOWLEDGMENTS

Authors of this study would like to thank College of Veterinary Medicine, University of Baghdad-Iraq for their support.

NOVELTY STATEMENT

The novelty of the current study was to illustrate the role of Curcumin selenium nanoparticles in decreasing the adverse effects of anticancer drugs on female reproductive system by modulating folliculogenesis and expression of the VEGE gene of rats ovary.

AUTHOR'S CONTRIBUTIONS

Baraa Najim was responsible for designing the experiment. Rawya Shakir conducted data analysis and experimental procedures. Besides, Baraa Najim wrote the article, interpretation and also provided conceptual advice.

Conflict of Interest

No conflict of interest are declared by authors for the contents of the manuscript.

REFERENCES

Al-Ebadi WA, Al-Awad HA, Bashi AM (2021). Preparation of Nanoparticles of Selenium/Zinc Oxide Reductase in an Environmentally Friendly Green Synthesis Method and Studying Their Effect on Pseudomonas Aeruginosa. Ann. Rom. Soc. Cell Biol., 6: 2650-61.

Alhealy EG, alkazzaz M, AL-Nuaimy WMT (2021). The Role of Selenium On Some Hormones And Histological Structures In Ovaries Of Hypothyroid Female Albino Rats. Ann. Coll. Med. Mosul, 43(1): 21-28.

Al-Kurdy MJ, KhudairK K (2020). Effect of selenium loaded Ribes nigrum nanoparticles on genetic markers in male rats with D-galactose induced toxicity. Online J. Vet. Res., 24(5): 312-327.

Wali AT, Alqayim MA (2019). Biosynthesis characterization and bioactivity of selenium nanoparticles synthesized by propolis. The Iraqi J. Vet. Med., 43(1): 197-209. https://doi.org/10.30539/iraqijvm.v43i1.490

Baarda B, van Dijkum C (2019). Introduction to Statistics with SPSS. Routledge. ISBN 90 207 32978.

Bhatia M, Bhalerao M, Cruz-Martins N, Kumar D (2021). Curcumin and cancer biology: Focusing regulatory effects in different signalling pathways. Phytother. Res., 35(9): 4913-

4929. https://doi.org/10.1002/ptr.7121
Carvalho LF, Silva AMF, Carvalho AA (2017). The use of antioxidant agents for chemotherapy-induced peripheral neuropathy treatment in animal models. Clinical and Experimental Pharm. Physiol., 44(10): 971-979. https://doi.org/10.1111/1440-1681.12803
Dulf PL, Mocan M, Coadă CA, Dulf DV, Moldovan R, Baldea I, Filip AG (2023). Doxorubicin-induced acute cardiotoxicity is associated with increased oxidative stress, autophagy, and inflammation in a murine model. Naunyn-Schmiedeberg's Arch. Pharmacol., 396(6): 1105-1115. https://doi.org/10.1007/s00210-023-02382-z
Elneklawi MS, Mohamed ZN, Hussein MA, Mohamad EA (2023). STEN ameliorates VEGF gene expression by improving XBP1/mRNA-21/mRNA-330 signaling pathways in cisplatin-induced uterus injury in rats. J. Drug Delivery Sci. Technol., 87: 104760. https://doi.org/10.1016/j.jddst.2023.104760
Fouda A, Hassan SE, Eid AM, Abdel-Rahman MA, Hamza MF (2022). Light enhanced the antimicrobial, anticancer, and catalytic activities of selenium nanoparticles fabricated by endophytic fungal strain, Penicillium crustosum EP-1. Sci. Rep., 12;12(1): 11834.
Gao Y, Wu T, Tang X, Wen J, Zhang Y, Zhang J, Wang S (2023). Increased cellular senescence in doxorubicin-induced murine ovarian injury: Effect of senolytics. Geroscience, 45(3):1775-1790. https://doi.org/10.1007/s11357-023-00728-2
Geoffrion LD, Hesabizadeh T, Medina-Cruz D, Kusper M, Taylor P, Vernet-Crua A, Guisbiers G (2020). Naked selenium nanoparticles for antibacterial and anticancer treatments. ACS omega, 5(6): 2660-2669. https://doi.org/10.1021/acsomega.9b03172
Giordano A, Tommonaro G (2019). Curcumin and cancer. Nutrients, 11(10):2376. https://doi.org/10.3390/nu11102376
Hutomo S, Susilowati H, Suryanto YI, Kurniawan C (2017). Perubahan morfologi sel HeLa setelah paparan ekstrak etanolik Curcuma longa. Majalah Kedokteran Gigi Indonesia, 2(1): 1-5. https://doi.org/10.22146/majkedgiind.11248
Jadaan, GH, Khudair, KK (2023). Curcumin phytosome as an anti-inflammatory and hypolipidemic in nano-silicon treated female rats . Adv. Anim. Vet. Sci., 11(12): 2023-2029. http://dx.doi.org/10.17582/journal.aavs/2023/11.12.2023.2029
Jadoun S, Arif R, Jangid NK, Meena RK (2021). Green synthesis of nanoparticles using plant extracts: A review. Environ. Chem. Lett., 19(1): 355-374. https://doi.org/10.1007/s10311-020-01074-x
Jaffar HI, Hussein SI (2015). Preparation and some characterization of curcumin-silica materials by sol-gel method. IJARSET, 6:1153-1160.
Jayarambabu N, Akshaykranth A, Rao TV, Rao KV, Kumar RR (2020). Green synthesis of Cu nanoparticles using Curcuma longa extract and their application in antimicrobial activity. Mater. Lett., 259: 126813.
Jalouli M, Mofti A, Elnakady YA, Nahdi S, Feriani A, Alrezaki A, Harrath, AH (2022). Allethrin promotes apoptosis and autophagy associated with the oxidative stress-related PI3K/AKT/mTOR signaling pathway in developing rat ovaries. Int. J. Mol. Sci., 23(12): 6397. https://doi.org/10.3390/ijms23126397
Khaledizade E, Tafvizi F, Jafari P (2024). Anti-breast cancer activity of biosynthesized selenium nanoparticles using Bacillus coagulans supernatant. J. Trace Elem. Med. Biol., 82: 127357. https://doi.org/10.1016/j.jtemb.2023.127357
Al-Kurdy MJ, Khudair KK (2020). Synthesis and characterization of black currant selenium nanoparticles (part I). https://doi.org/10.30539/ijvm.v44i2.974
Khudair K. K., Al-Kurdy, M.J. and Al-Kinani, L.H. (2020). Synthesis and Characterization of Black Currant Selenium Nanoparticles (Part I). The Iraqi J. Vet. Med., 44 (2): 25-34.
Liu S, Jia Y, Meng S, Luo Y, Yang Q, Pan Z (2023). Mechanisms of and potential medications for oxidative stress in ovarian granulosa cells: a review. Int. J. Mol. Sci., 24(11): 9205. https://doi.org/10.3390/ijms24119205
Menon S, Ks SD, Santhiya R, Rajeshkumar S, Kumar V (2018). Selenium nanoparticles: A potent chemotherapeutic agent and an elucidation of its mechanism. Colloids and Surfaces B: Biointerfaces, 170: 280-292. https://doi.org/10.1016/j.colsurfb.2018.06.006
Nasrollahzadeh M, Sajadi SM (2016). Green synthesis of Pd nanoparticles mediated by Euphorbia thymifolia L. leaf extract: catalytic activity for cyanation of aryl iodides under ligand-free conditions. J. Colloid Interface Sci., 469: 191-195
Palmerini MG, Nottola SA., Tunjung WAS, Kadowaki A, Bianchi S, Cecconi S, Macchiarelli G (2016). EGF-FSH supplementation reduces apoptosis of pig granulosa cells in co-culture with cumulus-oocyte complexes. Biochem. Biophys. Res. Commun., 481(1-2): 159-164. https://doi.org/10.1016/j.bbrc.2016.10.151
Pang X, Zhang Y, Shi X, Peng Z, Xing Y, Han J (2020). Hirudin reduces the expression of markers of the extracellular matrix in renal tubular epithelial cells in a rat model of diabetic kidney disease through the hypoxia-inducible factor-1α (HIF-1α)/vascular endothelial growth factor (VEGF) signaling pathway. Medical Science Monitor: Int. Med. J. Exp. Clin. Re., 26: e921894-1.
Patel SS, Acharya A, Ray RS, Agrawal R, Raghuwanshi R, Jain P (2020). Cellular and molecular mechanisms of curcumin in prevention and treatment of disease. Crit. Rev. food Sci. Nutr., 60(6): 887-939. https://doi.org/10.1080/10408398.2018.1552244
Peng Y, Ao M, Dong B, Jiang Y, Yu L, Chen Z, Xu R (2021). Anti-inflammatory effects of curcumin in the inflammatory diseases: Status, limitations and countermeasures. Drug Des. Dev. Ther., 4503-4525. https://doi.org/10.2147/DDDT.S327378
Pinto E, Pelizzaro F, Cardin R, Battistel M, Palano G, Bertellini F, Russo FP (2024). HIF-1α and VEGF as prognostic biomarkers in hepatocellular carcinoma patients treated with transarterial chemoembolization. Dig. Liver Dis., 56(5): 872-879. https://doi.org/10.1016/j.dld.2023.09.019
Refaie MM, El-Hussieny M, Abdel-Hakeem EA, Fawzy MA, Mahmoud Abd El Rahman ES, Shehata S (2022). Phosphodiesterase inhibitor, Vinpocetine, guards against doxorubicin induced cardiotoxicity via modulation of HIF/VEGF and cGMP/cAMP/SIRT signaling pathways. Hum. Exp. Toxicol., 41: 09603271221136209.
Regulska K, Regulski M, Karolak B, Murias M, Stanisz B (2019). Can cardiovascular drugs support cancer treatment? The rationale for drug repurposing. Drug Discov. Today, 24(4): 1059-1065. https://doi.org/10.1016/j.drudis.2019.03.010
Sabea AM, Al-Qaiym MA (2023). Selenium synergize levothyroxine in restoring leukocytes cluster differentiation expression in methimazole induced hypothyroidism. Adv.

Anim. Vet. Sci., 11(10):1681-1689.

Salim AG, Hasan HF (2022). The role of Avena sativa seeds alcoholic extract and enalapril against doxorubicin-induced cardiac toxicity in female rats. Biochem. Cell. Arch., 22(1): 2153-2161. https://connectjournals.com/03896.2022.22.2153

Samare-Najaf M, Zal F, Safari S (2020). Primary and secondary markers of doxorubicin-induced female infertility and the alleviative properties of quercetin and vitamin E in a rat model. Reprod. Toxicol., 96: 316-326. https://doi.org/10.1016/j.reprotox.2020.07.015

Schmittgen TD, Livak KJ (2008). Analyzing real-time PCR data by the comparative CT method. Nature protocols, 3(6): 1101-1108. https://doi.org/10.1038/nprot.2008.73

Shareef BQ, Al Qadhi HI, Shayma'a AJ (2024). Antioxidant Effects of Selenium Nanoparticles Prepared from Eruca Sativa Extract on Ketoconazole–Induced Testicular Oxidative Damage in Male Rats. J. Fac. Med. Baghdad, 66(1): 58-66. https://doi.org/10.32007/jfacmedbagdad.6612174

Soleimani V, Sahebkar A, Hosseinzadeh H (2018). Turmeric (*Curcuma longa*) and its major constituent (curcumin) as nontoxic and safe substances. Phytother. Res., 32(6): 985-995.

Soleimani R, Heytens E, Darzynkiewicz Z, Oktay K (2011). Mechanisms of chemotherapy-induced human ovarian aging: double strand DNA breaks and microvascular compromise. Aging (Albany NY), 3(8): 782.

Sood MA, Khudiar KK (2019). Role of Salvia officinal's silver nanoparticles in attenuating renal damage in rats exposed to methotrexate (Part I). 42(2): 7-20 https://doi.org/10.30539/iraqijvm.v42i2.281

Suad KA, Al-Shamire JSH, Dhyaa AA (2018). Histological and biochemical evaluation of supplementing broiler diet with β-hydroxy-methyl butyrate calcium (β-HMB-Ca). Iran. J. Vet. Res., 19(1) :27- 34. https://doi.org/10.22099/ijvr.2018.4764

Suvarna KS, Layton C, Bancroft JD (2018). Bancroft's theory and practice of histological techniques E-Book. Elsevier health sciences. ISBN: 978-0-7020-6864-5

Torres-Ruiz S, Tormo E, Garrido-Cano I, Lameirinhas A, Rojo F, Madoz-Gúrpide J, Eroles P (2023). High VEGFR3 expression reduces doxorubicin efficacy in triple-negative breast cancer. Int. J. Mol. Sci., 24(4): 3601. https://doi.org/10.3390/ijms24043601

Ungurianu A, Zanfirescu A, Margină D (2022). Regulation of gene expression through food—Curcumin as a sirtuin activity modulator. Plants, 11(13): 1741. https://doi.org/10.3390/plants11131741

Walsh KA, Kastrappis G, Fifis T, Paolini R, Christophi C, Perini MV (2022). SAR131675, a VEGRF3 Inhibitor, Modulates the Immune Response and Reduces the Growth of Colorectal Cancer Liver Metastasis. Cancers, 14(11): 2715. https://doi.org/10.3390/cancers14112715

Wang Y, Liu M, Johnson SB, Yuan G, Arriba AK, Zubizarreta ME, Xiao S (2019). Doxorubicin obliterates mouse ovarian reserve through both primordial follicle atresia and overactivation. Toxicol. Appl. Pharm., 381: 114714. https://doi.org/10.1016/j.taap.2019.114714

Xiao S, Zhang J, Liu M, Iwahata H, Rogers HB, Woodruff TK (2017). Doxorubicin has dose-dependent toxicity on mouse ovarian follicle development, hormone secretion, and oocyte maturation. Toxicol. Sci., 157(2): 320-329. https://doi.org/10.1093/toxsci/kfx047

Yang X, Wang W, Zhang Y, Wang J, Huang F (2019). Moxibustion improves ovary function by suppressing apoptosis events and upregulating antioxidant defenses in natural aging ovary. Life Sci., 229: 166-172. https://doi.org/10.1016/j.lfs.2019.05.040

Zhang T, Qi M, Wu Q, Xiang P, Tang D, Li Q (2023). Recent research progress on the synthesis and biological effects of selenium nanoparticles. Front. Nutr., 10: 1183487. https://doi.org/10.3389/fnut.2023.1183487

Zhou N, Long H, Wang C, Yu L, Zhao M, Liu X (2020). Research progress on the biological activities of selenium polysaccharides. Food Funct., 11(6): 4834-4852. https://doi.org/10.1039/C9FO02026H